Progress in Agricultural Engineering Sciences 21 (2025) 1, 233–252
DOI: 10.1556/446.2025.00194

1828
AKADÉMIAI KIADÓ

# Study of relative humidity with Markov chains in the Tokaj-Hegyalja wine region

D. SZÁM[1,2*], ZS. HETESI[3,4], A.P. TAKÁCS[5] and G. KEVE[1]

[1] Department of Regional Water Management, Faculty of Water Sciences, Ludovika University of Public Service, 6500 Baja, Hungary

[2] Institute of Biology, Faculty of Natural Sciences, University of Pécs, 7624 Pécs, Hungary

[3] Department of Water and Environmental Security, Faculty of Water Sciences, Ludovika University of Public Service, 6500 Baja, Hungary

[4] Faculty of Natural Sciences, Institute of Mathematics and Informatics, University of Pécs, 7624, Pécs, Hungary

[5] Department of Plant Protection, Institute of Plant Protection, Hungarian University of Agriculture and Life Sciences, Georgikon Campus, 8360 Keszthely, Hungary

## ORIGINAL RESEARCH PAPER

Received: March 4, 2025 • Accepted: July 23, 2025
Published online: August 20, 2025


### ABSTRACT

The aim of our research is to contribute to the modeling of relative humidity with Markov chains and its use in crop protection forecasting in the Tokaj-Hegyalja wine region. The two most common wine grape varieties in this region are *Vitis vinifera* cv. Furmint and *V. vinifera* cv. Hárslevelű. For noble rot on these varieties, humidity in the optimum range is an essential environmental condition. Using 10-min and 60-min resolution humidity data sets from the Hungarian Meteorological Service (HungaroMet) for the period 2002–2020, we estimated the probability that a random humidity measurement will fall into a given result (five humidity categories) in the future. The mathematical model used for this research is the theory of Markov chains, a new approach to statistical analysis of relative humidity data. It is pointed out that the Markov process of relative humidity variation and the results of a 60-min resolution data series across 19 years of study can be used to model humidity.

### KEYWORDS

relative humidity, Markov chains, Tokaj-Hegyalja, *Vitis vinifera*, noble rot

* Corresponding author. E-mail: szam.dorottya.reka@gmail.com

## 1. INTRODUCTION AND REVIEW OF LITERATURE

The Tokaj-Hegyaljai wine region is the only wine region in Hungary that has been on the World Heritage List since 2002 due to its unique natural features and several centuries-old grape and wine cultures (Szepesi et al., 2017).

In the wine region, the law regulates the range of varieties that can be planted, all of which are white grape varieties with excellent varietal characteristics and noble rotting (Dékány et al., 2010). The two largest area shares are cv. Furmint (66%) and cv. Hárslevelű (19%). These two varieties are the most susceptible to noble rot, and their sweet botrytized wines are internationally recognized (Echikson, 2006; Kerridge et al., 2004).

The noble rot of grapes is a unique feature of winemaking that is facilitated by favorable mesoclimatic conditions, soil conditions, and fungal communities under appropriate ripening conditions (Magyar, 2011). From fruit setting to harvest, the surface of healthy grapes is rich in fungal communities. Fungi belonging to the genera *Aureobasidium*, *Cladosporium*, *Hanseniaspora*, *Metschnikowia*, *Penicillium*, *Rhodotorula* and *Botrytis* are present (Hegyi-Kaló et al., 2020). Among them, the *Botrytis cinerea* fungi species complex of the genus *Botrytis* plays a prominent role, appearing on the surface of grapes after the onset of veraison (ripening). The majority of studies have shown that *B. cinerea* fungi are the primary contributors to noble rot. This species complex is the one that, after its emergence, gradually displaces other filamentous fungi and becomes dominant by harvest (Hegyi-Kaló et al., 2017).

The role of mesoclimates in noble rot, focusing on *B. cinerea*, is emphasized in several studies. They point out that the beneficial effects of the fungus are typical in wine regions with a suitable mesoclimate; for example, in Sauternes AOC Bordeaux and Selection de Grains Nobles in France, where noble rot is called pourriture noble. Germany and Austria also have long-established sweet wine regions (Rheingau region, Burgenland) that are the result of ideal conditions for noble rot (Edelfäule). In Hungary, conditions are ideal in the Tokaj-Hegyalja wine region (Amerine et al., 2020; Cioch et al., 2021; Elmer et al., 2007).

All weather elements play a decisive role in the ideal mesoclimate for noble rot. The importance of two of these elements (precipitation and humidity) is highlighted in many studies although they are difficult to analyze separately due to strong cross-correlations (Sunarmi, 2022). The role of relative humidity as a weather element is important because the conidia formation of *B. cinerea* is highly humidity-dependent. One experiment at a constant temperature of 20 °C between 65.5% and 100% relative humidity showed that conidia formation exhibits a maximum curve, reaching the optimum at around 85% relative humidity. At higher relative humidity, conidia formation shows a slight tendency to decrease (Ciliberti et al., 2016; Mesterházy et al., 2014).

The neighborhood of the Tisza and Bodrog rivers provides the humidity in specific ranges required for noble rot and the production of botrytis wines in the Tokaj-Hegyalja wine region. On the other hand, the geomorphology of the mountain area (wind sheltered basins) contributes to the high humidity levels. An increase in altitude of 100 m in the mountainous terrain results in an increase in annual precipitation of about 35 mm (Hungarian Meteorological Service, 2021).

However, the mesoclimate (with humidity in a specific range) is under severe threat from the effects of climate change: more extreme precipitation patterns, more frequent drought periods. In order to maintain the security of the harvest, it is essential to develop a climate adaptation strategy, make up for lost rainfall in a planned way, and even use artificial humidification. As early as 1959, the artificial reproduction of weather conditions for noble rot were being investigated. Experiments have been conducted with artificial inoculation of harvested grape berries (Nelson and Nightingale, 1959), spraying of laboratory-prepared fungal suspensions (Magyar, 2011), artificial botrytized grape juice (Wang et al., 2017), and artificial humidification.

Advantageously, Hungarian viticulture is a sector for which there is considerable export demand. This and the relatively high average cost of cultivation per hectare compared to other fruit crops, especially intensive trellis cultivation (Hungarian Ministry of Interior, 2021) justify the crop's high market value. The high prices at sale are an incentive for innovation, and grapes are one of the fruit crops where weather forecasting-based crop protection solutions and weather forecasting modeling software are also being used internationally.

The objective of our research was to develop a mathematical model that provides a simple, low-data-capacity, accurate prediction of relative humidity trends. Our goal, beyond the scope of our manuscript, is to make this model suitable for integration into a crop protection forecasting software. The software will indicate to farmers the timing and need for crop protection interventions. Our results can help improve the accuracy of crop protection forecasting in practice, reduce pesticide use and environmental impact, and save costs. Accurate weather forecasting is the basis of modern integrated pest management. The model we have developed can be adapted to other pathogens and crops, in addition to *Botrytis* species, where humidity is also a key factor in the establishment of infection.

## 2. MATERIALS AND METHODS

### 2.1. Study area and datasets

The Tokaj-Hegyalja in northern Hungary is an area of 88,124 ha in Borsod-Abaúj-Zemplén county, comprising 27 municipalities (Fig. 1). The area is bordered by Kopasz Hill in Tokaj to the south, by Sátor Hill in Abaújszántó to the north-west, and the third vertex is at the north-eastern corner of Sátoraljaújhely (Hungarian Central Statistical Office, 2016).

For our study, we used relative humidity data from the Hungarian Meteorological Service station 62,612 (HungaroMet, 2023), located on the border of the Tarcal municipality in the Tokaj-Hegyalja wine region.

The relative humidity was measured from autumn (1 September) after veraison until harvest (31 October). This is a difficult time interval to define, depending on the vintage, as the ripening process is obviously influenced by weather and agrotechnical aspects (e.g., multiple harvests), as discussed in more detail in the introduction. Furthermore, cv. Furmint and cv. Hárslevelű are very late-ripening varieties (Pulliat, 1897). There can be a difference of up to one month in ripening time between two vintages. Their ripening each year is not even possible without the necessary amount of growing-season heat. Thus, the vintage effect is more pronounced than in the case of early- and medium-maturing varieties (Rakonczás, 2014). However, for our study, we needed a uniform maturation time, which we obtained from published data. In the case of cv. Furmint, the berries reach biological maturity in mid- to late-October, whereas in the case of cv. Hárslevelű, the berries reach biological maturity in the first half of October.

We processed 19 years of relative humidity data from 2002 to 2020 at 10 and 60 min resolutions. 2020 was the last year for which we had a complete set of HungaroMet data for

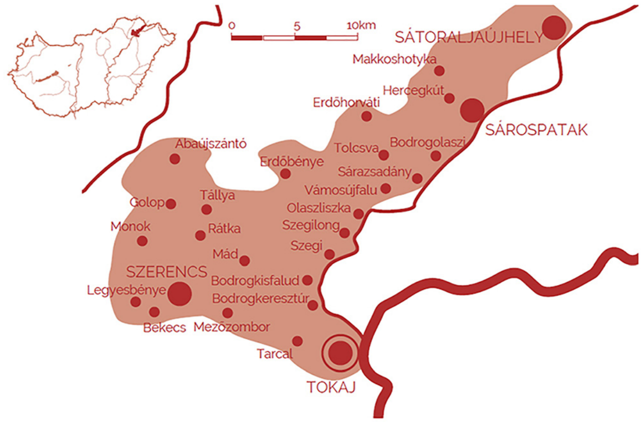


*Fig. 1.* The Tokaj-Hegyalja wine region examined in the manuscript includes the settlements of Tarcal and Sátoraljaújhely, where the weather measuring stations are located. (Own source)

the period under study. No outliers or data gaps were detected, so no data deletion or imputation preceded our data analysis.

The study area is located in the mountains of the Tokaj-Hegyalja wine region, which forms a geographical unit, from which the homogeneity of the weather data would follow according to our hypothesis, but we wanted to be sure of the area-dependent effect of the weather forecasts for the region. In the region, HungaroMet operates only two automatic measuring stations, which provide data series on relative humidity between 2002 and 2020 without any shortage of data. Since relative humidity shows a close correlation with precipitation and temperature, we also compared these variables. Precipitation and temperature are also typical parameters for the development of meteorological droughts, and their investigation can be important for this reason.

One of the measuring stations is located on the border of the city of Tarcal (GPS coordinates: N 48.145°, E 21.3344°), the other one is approximately 36 km away in Sátoraljaújhely (GPS coordinates: N 48.3808°, E 21.6589°). We used complete data files from the two automatic measuring stations. We filtered out three parameters: relative humidity, daily maximum temperatures and daily precipitation totals. The distribution of the data was compared by year using the two-sample Kolmogorov-Smirnov test. When applying these tests, we chose a lower significance level ($\alpha = 0.001$) because it is a more robust, weaker statistical test (Marozzi, 2009, 2013). We chose this test because the preliminary normality tests (Shapiro–Wilk tests) without exception showed significant deviations from normality in the case of the $2 \times 19$ sample pairs. There are also indications in the literature that daily precipitation totals within a year are not normally distributed (Ferreira and Lemeshko, 2021; Wilks, 1989). This is also true for the distribution of daily maximum temperatures within the year.

## 2.2. Using the Markov chain

The Markov property means that in a chain of events, knowledge of the present is sufficient to determine the probability of the next step, knowledge of previous steps or states does not provide new information, the Markov chain is memoryless. This means that if we know the current state of the process, we do not need additional information about past states to make the best possible prediction about the probability of the next step. When the current state allows us to infer the next step in the sequence, we speak of a first-order Markov chain (Karlin and Taylor, 1985; Kontur, 1993; Markov, 1906; Seneta, 1966).

Markov chains are useful in the statistical analysis of a variety of weather events. They have been used to predict the daily temperature change (Hussein et al., 2024), probability of drought (Fekete, 2022; Freidoni et al., 2015; Szám et al., 2024), forest fires (Martell, 1999), wet and dry patterns of daily precipitation observed (Sonnadara and Jayewardene, 2014), daily and monthly rainfall sums (Fekete and Keve, 2020; Ibeje et al., 2018; Tettey et al., 2017). However, to the best of our knowledge, they have not yet been used to analyze relative humidity data.

We applied the Markov model in two ways. First, we examined the short-term (10 min) and second-time long-term (60 min) variability of relative humidity. For Markov chains, given all possible outputs *(1,2,…,i,…,n)*, we can give the probability of where the chain will end up in the next step. Formally, $p_{ij}$ is the probability that the chain moves from state $i$ to state $j$ in the next step, i.e. the entire chain can be described by a matrix where the $ij$-th element is $p_{ij}$. To construct the matrix, we need to know the frequency of steps between the elements of the chain, from which we form a probability. From the HungaroMet data series, limiting probabilities were established. Relative humidity values were classified into five categories (in brackets to denote the condition used later):

- very dry weather period ($R_1$): RH% $\leq$ 60
- dry weather period ($R_2$): 60 $<$ RH% $\leq$ 70
- average weather period ($R_3$): 70 $<$ RH% $\leq$ 80
- humid weather period ($R_4$): 80 $<$ RH% $\leq$ 90
- very humid weather period ($R_5$): 90 $<$ RH%

The transition matrix for the autumn of a given year was generated as follows. Based on the measurements from HungaroMet, we examined the value of humidity that follows a given time interval. If a humidity class $i$ {1,…,5} was measured in a given measurement and $j$ {1,…,5} in the next measurement, the element $r_{ij}$ of the transition matrix increases by one. State 1 is defined as very dry weather, while state 5 is defined as very humid weather. Our transition matrix for a given year is then:

$$\begin{pmatrix} r_{11} & r_{12} & r_{13} & r_{14} & r_{15} \\ r_{21} & r_{22} & r_{23} & r_{24} & r_{25} \\ r_{31} & r_{32} & r_{33} & r_{34} & r_{35} \\ r_{41} & r_{42} & r_{43} & r_{44} & r_{45} \\ r_{51} & r_{52} & r_{53} & r_{54} & r_{55} \end{pmatrix} \tag{1}$$

Following the above methodology, we calculated from the transition matrix (Eq. (1)) for each year and then determined the limiting distribution. The limiting distribution describes the probabilities of being in each state after a large number of transitions, regardless of the initial state, provided the chain converges and it is computed by taking the limit of the powers of the transition matrix as the number of steps approaches infinity. The limiting distribution could be calculated by successive multiplications of the transition matrix itself (Dobrow, 2016; Ross, 2010), we followed this methodology.

## 3. RESULTS

Appendix 1 contains the transition probability matrices for the humidity study, and Table 1 the limiting distributions for the period 2002−2020 based on 10-min resolution data at the Tarcal monitoring station. The average of the $P_5$ limiting probabilities for the period with humidity above 90% in Table 1 is 17.43%, which means that our calculations indicate that the average probability of relative humidity exceeding 90% in the future for a randomly selected 10-min measurement is about the same. The probability of exceeding 80% is 35.07%.

The values of the limit distributions $P_1$, $P_2$, $P_3$, $P_4$, $P_5$ are shown in Fig. 2. From the Shapiro–Wilk tests, which can be applied to small sample sizes, it can be concluded that the values obtained over the 19-year period follow a normal distribution even when slight outliers are taken into account, i.e., the probability of these humidity Markov transitions can be characterized by a given mean and standard deviation. The values of the two extreme transitions ($P_1$ and $P_5$) show the largest variance. For $P_5$, the variance is an order of magnitude larger compared to $P_2$, $P_3$, $P_4$.

Appendix 2 contains the transition probability matrices for the humidity study, and Table 2 contains the limiting distributions for the period 2002−2020 based on the 60-min resolution data of the Tarcal monitoring station. The average of the $P_5$ limiting probabilities for the period with humidity above 90% in Table 2 is 17.56%, which means that in the future, on average, the probability of relative humidity exceeding 90% for a randomly selected 60-min measurement is the same. The probability of exceeding 80% is 35.05%.

*Table 1.* Limiting distributions for the relative humidity test for the period 2002−2020 calculated from the 10-min resolution data series at the Tarcal monitoring station

| Year | $P_1$ | $P_2$ | $P_3$ | $P_4$ | $P_5$ |
|---|---|---|---|---|---|
| 2002 | 0.174 | 0.093 | 0.148 | 0.185 | 0.401 |
| 2003 | 0.303 | 0.176 | 0.184 | 0.186 | 0.150 |
| 2004 | 0.254 | 0.173 | 0.187 | 0.174 | 0.212 |
| 2005 | 0.221 | 0.202 | 0.233 | 0.219 | 0.125 |
| 2006 | 0.362 | 0.236 | 0.212 | 0.140 | 0.050 |
| 2007 | 0.298 | 0.189 | 0.217 | 0.221 | 0.075 |
| 2008 | 0.229 | 0.240 | 0.243 | 0.228 | 0.060 |
| 2009 | 0.382 | 0.179 | 0.149 | 0.174 | 0.115 |
| 2010 | 0.169 | 0.191 | 0.214 | 0.208 | 0.218 |
| 2011 | 0.417 | 0.215 | 0.196 | 0.127 | 0.045 |
| 2012 | 0.263 | 0.173 | 0.227 | 0.168 | 0.170 |
| 2013 | 0.319 | 0.201 | 0.166 | 0.137 | 0.177 |
| 2014 | 0.138 | 0.162 | 0.198 | 0.197 | 0.304 |
| 2015 | 0.260 | 0.168 | 0.188 | 0.172 | 0.212 |
| 2016 | 0.230 | 0.189 | 0.178 | 0.210 | 0.193 |
| 2017 | 0.202 | 0.166 | 0.192 | 0.196 | 0.244 |
| 2018 | 0.445 | 0.222 | 0.166 | 0.094 | 0.073 |
| 2019 | 0.311 | 0.223 | 0.187 | 0.147 | 0.132 |
| 2020 | 0.194 | 0.141 | 0.141 | 0.169 | 0.355 |

Own source.

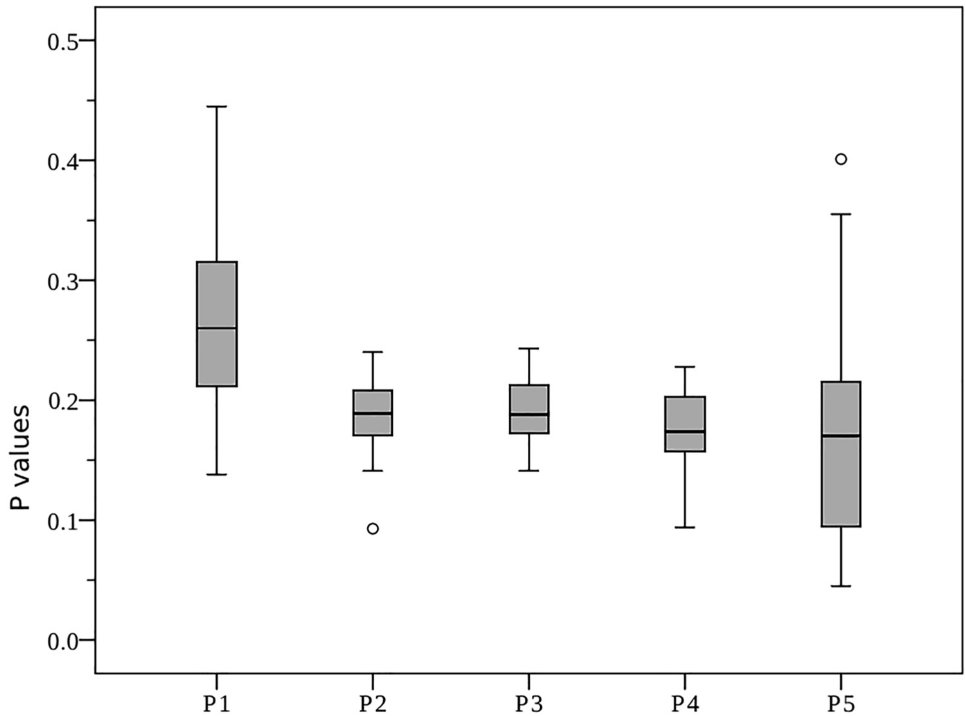


*Fig. 2.* Limiting distributions $P_1$, $P_2$, $P_3$, $P_4$, $P_5$ for the relative humidity test over the period 2002−2020 calculated from the 10-min resolution data series. The circles mark the outliers. (Own source)

In order to validate the model of using a Markov chain in the investigation of humidity, a Monte Carlo simulation was used to simulate the annual vapor data series and to construct the transition matrices (see Fig. 3).

For each year, we examined the distribution that best describes the histogram of hourly humidity data for that year. Of the distributions of interest, the best fit was found for the Weibull distribution (Ferreira and Lemeshko, 2021; Wilks, 1989). The Weibull distribution was first identified by the French mathematician René Maurice Fréchet, and then described in detail by the Swedish mathematician Waloddi Weibull in 1939 (Weibull, 1939). The Weibull distribution has since been shown to model a wide range of random variables, largely the nature of the time to failure or the time between events (Kupolusi and Akindolani, 2024). Using this distribution, 10 Monte Carlo simulations were run each year using Julius AI. In this simulation, we used the empirical cumulative distribution function (CDF) of the observed humidity data as a basis, since the true density function and distribution were unknown (Dobrow, 2016, Ch. 5). From this empirical CDF, we generated random humidity sequences via inverse transform sampling. Then, using the resulting discrete humidity states, we constructed synthetic time series by sampling transitions according to the estimated Markov transition matrix. Each simulation reproduced the typical distributional shape of the autumn humidity record. Figure 3 shows the cumulative distributions of ten simulated series performed for the year 2011

*Table 2.* Limiting distributions for the relative humidity test for the period 2002−2020 calculated from the 60-min resolution data series at the Tarcal monitoring station

| Year | $P_1$ | $P_2$ | $P_3$ | $P_4$ | $P_5$ |
|---|---|---|---|---|---|
| 2002 | 0.174 | 0.093 | 0.148 | 0.185 | 0.401 |
| 2003 | 0.303 | 0.174 | 0.187 | 0.184 | 0.152 |
| 2004 | 0.257 | 0.171 | 0.187 | 0.170 | 0.215 |
| 2005 | 0.223 | 0.205 | 0.224 | 0.221 | 0.127 |
| 2006 | 0.365 | 0.240 | 0.205 | 0.145 | 0.045 |
| 2007 | 0.299 | 0.184 | 0.221 | 0.221 | 0.074 |
| 2008 | 0.229 | 0.238 | 0.250 | 0.222 | 0.061 |
| 2009 | 0.384 | 0.178 | 0.153 | 0.167 | 0.118 |
| 2010 | 0.169 | 0.193 | 0.211 | 0.209 | 0.217 |
| 2011 | 0.412 | 0.216 | 0.201 | 0.126 | 0.045 |
| 2012 | 0.261 | 0.167 | 0.230 | 0.172 | 0.171 |
| 2013 | 0.322 | 0.202 | 0.169 | 0.130 | 0.177 |
| 2014 | 0.139 | 0.163 | 0.196 | 0.200 | 0.302 |
| 2015 | 0.259 | 0.166 | 0.190 | 0.171 | 0.215 |
| 2016 | 0.229 | 0.186 | 0.180 | 0.207 | 0.197 |
| 2017 | 0.201 | 0.163 | 0.194 | 0.195 | 0.247 |
| 2018 | 0.445 | 0.227 | 0.161 | 0.093 | 0.074 |
| 2019 | 0.309 | 0.221 | 0.193 | 0.141 | 0.136 |
| 2020 | 0.191 | 0.143 | 0.137 | 0.176 | 0.354 |

Own source.

compared to the original data. For each year, we calculated the limiting distribution based on the simulated data and obtained values of $P_1$, … $P_5$. The close match between the simulated and observed distributions supports the validity of the Markov chain model in capturing the overall statistical behavior of humidity.

We found that the steady-state distributions from 10-min and 60-min resolution humidity data are nearly identical. This means that, on average for a year, it is irrelevant for weather modeling whether the time resolution is 10 or 60 min. In other words, either in the case of collecting the data or using the software for modeling, it is sufficient to use 60-min resolution data series, which reduces the amount of data to be processed for sixth part.

The year-to-year variation in the limiting distributions $P_1$, $P_2$, $P_3$, $P_4$, $P_5$ for the 10-min and 60-min resolution data series cannot be said to show significant trend-like changes. The values of the limiting distribution $P_1$, $P_2$, …, $P_5$ calculated for consecutive years were subjected to normality tests per column and the result was that all columns $P_i$ are normally distributed, see Table 3 for the parameters of the fitted distributions. The skewness of the distributions is shown in the boxplot in Fig. 2, sproving that the skewness of the distributions is minimal.

However, it is possible that a different result would be obtained if this effect, which we hypothesize to be due to climate change, were examined over a time series longer than 19 years.

The following was established about the spatial validity of the application of Markov chains. The distribution of the daily maximum temperature at the two measuring stations examined did not differ significantly (Table 4). However, significant differences emerged in the case of daily precipitation (Table 5) and relative humidity (Table 6). In other words, the latter two variables

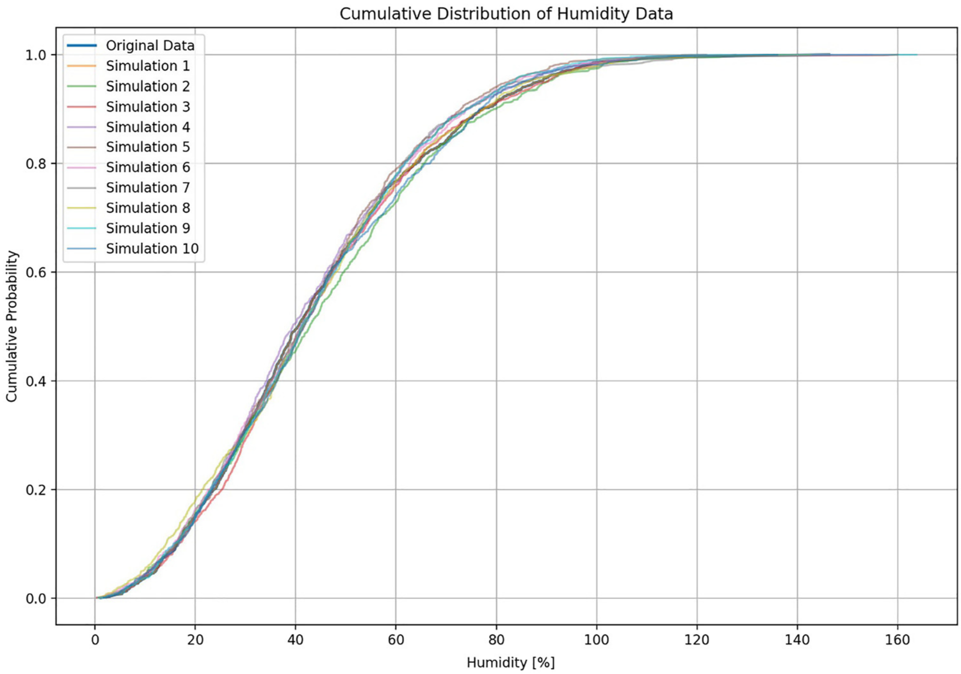


*Fig. 3.* Monte Carlo simulation of humidity data with 60 min time resolution. The cumulative distribution of the humidity in year 2011: original data (blue), simulated data: various colors. (Own source) (For the colour figure, see the online version)

*Table 3.* Normality test of the annual limiting distributions $P_1$, $P_2$, $P_3$, $P_4$, $P_5$ using the Shapiro–Wilk test for the period 2002–2020 calculated from the 10-min resolution data series

| Sample | Statistic | df | Sig. | Mean | Variance |
|---|---|---|---|---|---|
| $P_1$ | 0.965 | 19 | 0.682 | 0.272 | 0.007 |
| $P_2$ | 0.944 | 19 | 0.305 | 0.186 | 0.001 |
| $P_3$ | 0.972 | 19 | 0.817 | 0.191 | 0.001 |
| $P_4$ | 0.960 | 19 | 0.572 | 0.176 | 0.001 |
| $P_5$ | 0.937 | 19 | 0.235 | 0.174 | 0.010 |

Own source.

show greater spatial variability, and their investigation requires denser measuring station coverage in the wine region.

## 4. DISCUSSION

The prediction of relative humidity with Markov chains is a novelty in our manuscript; to our knowledge, it has not been applied by others. However, the results of our manuscript are worth

*Table 4.* Comparison of the distribution of daily maximum temperatures measured at Tarcal and Sátoraljaújhely stations using two-sample Kolmogorov–Smirnov tests. Designation of significance level: $^{***}P = 0.001$

| Year | Different distribution | Sig. level | Year | Different distribution | Sig. level |
|---|---|---|---|---|---|
| 2002 | no | *** | 2012 | no | *** |
| 2003 | no | *** | 2013 | no | *** |
| 2004 | no | *** | 2014 | no | *** |
| 2005 | no | *** | 2015 | no | *** |
| 2006 | no | *** | 2016 | no | *** |
| 2007 | no | *** | 2017 | no | *** |
| 2008 | no | *** | 2018 | no | *** |
| 2009 | no | *** | 2019 | no | *** |
| 2010 | no | *** | 2020 | no | *** |
| 2011 | no | *** | | | |

Own source.

*Table 5.* Comparison of the distribution of precipitation data measured at Tarcal and Sátoraljaújhely stations using two-sample Kolmogorov–Smirnov tests. Designation of significance level: $^{***}P = 0.001$

| Year | Different distribution | Sig. level | Year | Different distribution | Sig. level |
|---|---|---|---|---|---|
| 2002 | yes | *** | 2012 | no | *** |
| 2003 | yes | *** | 2013 | yes | *** |
| 2004 | yes | *** | 2014 | no | *** |
| 2005 | no | *** | 2015 | yes | *** |
| 2006 | yes | *** | 2016 | no | *** |
| 2007 | yes | *** | 2017 | yes | *** |
| 2008 | yes | *** | 2018 | yes | *** |
| 2009 | no | *** | 2019 | yes | *** |
| 2010 | yes | *** | 2020 | yes | *** |
| 2011 | yes | *** | | | |

Own source.

comparing with other methods and models used to predict humidity. This comparison requires further research, which is beyond the scope of this manuscript. As with most weather prediction models, the application of artificial intelligence is at the forefront of research. Several studies have been published on the prediction of relative humidity using artificial intelligence (Lagrazon et al., 2023).

The results reported in our manuscript may also contribute to the investigation of artificial noble rot wine making. Maintaining a stable relative humidity over a long period is one of the essential conditions for artificial humidification processes. Artificial humidification is also done in plantations and laboratory conditions (Lorenzini et al., 2012; Negri et al., 2017; Tosi et al., 2013) to make noble rot wines.

Another question worthy of further research is whether predicting relative humidity using Markov methods can help predict the dew point. The exact mathematical relationship between

*Table 6.* Comparison of the distribution of daily average relative humidity measured at Tarcal and Sátoraljaújhely stations using two-sample Kolmogorov–Smirnov tests. Designation of significance level: $^{***}P = 0.001$

| Year | Different distribution | Sig. level | Year | Different distribution | Sig. level |
|---|---|---|---|---|---|
| 2002 | yes | *** | 2012 | no | *** |
| 2003 | yes | *** | 2013 | yes | *** |
| 2004 | yes | *** | 2014 | no | *** |
| 2005 | yes | *** | 2015 | yes | *** |
| 2006 | yes | *** | 2016 | yes | *** |
| 2007 | yes | *** | 2017 | yes | *** |
| 2008 | yes | *** | 2018 | yes | *** |
| 2009 | yes | *** | 2019 | yes | *** |
| 2010 | yes | *** | 2020 | yes | *** |
| 2011 | yes | *** | | | |

Own source.

relative humidity and dew point has been investigated in several studies (Lawrence, 2005). Knowledge of the conversion can be helpful in all applications (including agriculture) where the dew point is applied instead of relative humidity.

## 5. CONCLUSION

Monitoring humidity as a weather parameter with a significant influence on *Botrytis cinerea* infection is important. Markov processes cannot generally be used for probabilistic forecasting in the case of a limiting distribution. However, when the one-step transition matrix is used to predict the next daily weather event, a significantly more accurate probabilistic estimate than the frequency from a multi-year data series can be made. As we increase the power of the matrix, i.e. move away from the present, this advantage disappears and the limiting distribution converges to the probability calculated from the frequency.

Currently, the highest resolution relative humidity datasets available are at 10-min resolution. The question is whether such frequent measuring is necessary over a shorter period (e.g., a year or a period of drought). This can be addressed by examining whether the probability of a step-by-step change in the 10-min series is the same as the probability of change for less frequent sampling. The probability of transitions is given by the one-step transition probability matrix, from which, in the appropriate case, a stationary distribution of probabilities – in this case, the classes of change in humidity – can be obtained as a limit, which is a row vector. If the distribution of changes obtained from a 10-min sample and the hourly distribution of changes can be considered identical, two points are confirmed: first, it is not necessary to take a 10-min sample, a stationary distribution of sufficient quality can be obtained from an hourly sample; and second, that, probably, the sub-sample of the 10-min sample and the hourly distribution of the original sample can be considered identical.

As can be seen in the analysis, a stationary distribution can be constructed from year to year, where the elements of the row vector $P(p_1, p_2, \ldots, p_n)$ in the same position in a given year show the probability of measuring a humidity data with the same value, chosen at random. Looking at the values at the same $p_i$ location from year to year, a normal distribution is obtained for the data series obtained over the last 19 years. This allows us to predict with a certain probability – reflecting the rules of the normal distribution – the probability of a certain $p_i$ value in a given year.

However, whether the normal distribution $\varphi p(i)(x)$ over the same elements of the row vectors plotted over the present data – $P(p_1, p_2, \ldots, p_n)$ – differs from the normal distribution $\chi q(i)(x)$ from the data for older data series (over $Q(q_1, q_2, \ldots, q_n)$ ), that is, whether the effect of climate change, for example, is noticeable in the secular data series, requires further research.

## REFERENCES

Amerine, M.A. and Singleton, V.L. (2020). The wines of Northern and Eastern Europe. In: Amrine, M.A. and Singleton, V.L. (Eds.), *Wine*. University of California Press, Berkeley, USA, pp. 222–234, https://doi.org/10.1525/9780520312654-018

Ciliberti, N., Fermaud, M., Roudet, J., Languasco, L., and Rossi, V. (2016). Environmental effects on the production of *Botrytis cinerea* conidia on different media, grape bunch trash, and mature berries. *Australian Journal of Grape and Wine Research*, 22(2): 262–270, https://doi.org/10.1111/ajgw.12217

Cioch, M., Semik-Szczurak, D., and Skoneczny, S. (2021). *Botrytis* and wine production. In: Joshi, V.K., and Ramesh, C.R. (Eds.), *Winemaking*. CRC Press, Boca Raton, Florida, USA, pp. 166–190.

Dékány, T. and Técsi, Z. (2010). *The tokaj wine region – a world heritage site*, 1st ed. Corvina, Budapest, Hungary, pp. 1–32.

Dobrow, R.P. (2016). *Introduction to stochastic processes with R*. John Wiley and Sons, New York, p. 505.

Echikson, W. (2006). *Noble rot: a bordeaux wine revolution*, 1st ed. W. W. Norton & Company, New York, USA, pp. 240.

Elmer, P.A., and Michailides, T.J. (2007). Epidemiology of *Botrytis cinerea* in Orchard and Vine Crops. In: Elad, Y., Williamson, B., Tudzynski, P., and Delen, N. (Eds.), *Botrytis: biology, pathology and control*. Springer, Dordrecht, USA, pp. 243–272.

Fekete, Á. and Keve, G. (2020). Examining rainfall totals and drought periods with Markov chains. *Hydrological Bulletin*, 100(4): 60–69.

Fekete, Á. (2022). Estimating the probability of flash flooding with a bivariate Markov chain. *Hydrological Bulletin*, 102(2): 41–49.

Ferreira, L.S. and Lemeshko, N. (2021). Best-fit probability distribution models for monthly rainfall of Northeastern Brazil. *Water Science & Technology*, 84(6): 1541–1552, https://doi.org/10.2166/wst.2021.263

Freidooni, F., Ataei, H., and Shahriars, F. (2015). Estimating the occurrence probability of heat wave periods using the Markov chain model. *Journal of Sustainability Development*, 8(2): 26–45, https://doi.org/10.5539/jsd.v8n2p26

Hegyi-Kaló, J., Lengyel, S., Szalóki, N., Szén, O., Juhász, Á., and Váczy, K.Z. (2017). Microbial ecology on grape berries of different botrytization phases. *Plant Protection*, 53(11): 507–512.

Hegyi-Kaló, J., Hegyi, Á.I., Geml, J., Zsófi, Z., Pálfi, X., and Váczy, K.Z. (2020). Physico-chemical characteristics and culturable microbial communities of grape berries change strongly during noble rot development. *Plants*, 9(12): 1809, https://doi.org/10.3390/plants9121809

Hungarian Central Statistical Office (2016). The world heritage Tokaj wine region, Available at: https://www.ksh.hu/docs/hun/xftp/idoszaki/pdf/tokaji_borvid.pdf.

Hungarian Meteorological Service. (2021).

Hungarian Meteorological Service. (2023).

Hungarian Ministry of Interior. (2021). Planning guide for the 2022 district start work programmes. Appendix 1.: Production and maintenance costs.

Hussein, M.M.F., Hamad, A.S., and Muhamad, S. (2024). Modeling and analysis of daily temperature using logistic regression and Markov chain. In: *International conference on accounting, business, economics and politics*, June 2024.

Ibeje, A.O., Osuagwu, J., and Onosakponome, R. (2018). A Markov model for prediction of annual rainfall. *Journal of Engineering and Applied Science*, 3(11): 1–5.

Karlin, S. and Taylor, H.M. (1985). *An introduction to stochastic modeling*, 1st ed. Gulf Publishing, London, UK, pp. 95–184.

Kerridge, G. and Gackle, A. (2004). *Vines for wines: a wine lover's guide to the top wine grape varieties*, 1st ed. Csiro Publishing, Collingwood, Australia, pp. 39–43.

Kontur, I. (1993). *Hidrológiai számítások*, 1st ed. Akadémiai Kiadó, Budapest, Hungary, pp. 507–508.

Kupolusi, J.A. and Akindolani, T. (2024). Optimal weibull distribution I for dose-response modelling of theophylline drug. *Annals of Biostatistics & Biometric Applications*, 5(5): 1–6, https://doi.org/10.33552/ABBA.2024.05.000624

Lagrazon, P.G.G., Japor, J.E.E., Susa, J.A.B., Abante, M.V. (2023). Comparative analysis of machine learning models for relative humidity prediction in the Philippines. In: *1st IEEE international conference 'Smart Technology (ICE-SMARTec)*, July 17–19 2023. Bandung, Indonesia. Not numbered volumes, pp. 72–77. https://doi.org/10.1109/ICE-SMARTECH59237.2023.10461954

Lawrence, M.G. (2005). The relationship between relative humidity and the dewpoint temperature in moist air: a simple conversion and applications. *Bulletin of the American Meteorological Society*, 86(2): 225–233, https://doi.org/10.1175/BAMS-86-2-225

Lorenzini, M., Azzolini, M., Tosi, E., and Zapparoli, G. (2012). Postharvest grape infection of *Botrytis cinerea* and its interactions with other molds under withering conditions to produce noble-rotten grapes. *Journal of Applied Microbiology*, 114: 762–770, https://doi.org/10.1111/jam.12075

Magyar, I. (2011). Botrytized wines. *Advances in Food and Nutrition Research*, 63: 147–206, https://doi.org/10.1016/B978-0-12-384927-4.00006-3 PubMed: 21867895

Markov, A.A. (1906). Rasprostranenie zakona bol'shih chisel na velichiny, zavisyaschie drug ot druga. *Izvestiya Fiziko-matematicheskogo obschestva pri Kazanskom universitete*, 15(2): 135–156.

Marozzi, M. (2009). Some notes ont the location-scale Cucconi test. *Journal of Nonparametric Statistics*, 21(5): 629–647, https://doi.org/10.1080/10485250902952435

Marozzi, M. (2013). Nonparametric simultaneous tests for location and scale testing: a comparison of several methods. *Communications in Statistics – Simulation and Computation*, 42(6): 1298–1317, https://doi.org/10.1080/03610918.2012.665546

Martell, D.L. (1999). A Markov chain model of day to day changes in the Canadian forest fire weather index. *International Journal of Wildland Fire*, 9(4): 265–273, https://doi.org/10.1071/WF00020

Mesterházy, I., Mészáros, R., and Pongrácz, R. (2014). The effects of climate change on grape production in Hungary. *Idojaras*, 118(3): 193–206.

Negri, S., Lovato, A., Boscaini, F., Salvetti, E., Torriani, S., Commisso, M., Danzi, R., Ugliano, M., Polverari, A., Tornielli, G.B., and Guzzo, F. (2017). The induction of noble rot (*Botrytis cinerea*) infection during postharvest withering changes the metabolome of grapevine berries (*Vitis vinifera* L., cv. Garganega). *Frontiers in Plant Science*, 21(8): 1–12, https://doi.org/10.3389/fpls.2017.01002

Nelson, K.E., and Nightingale, M.S. (1959). Studies in the commercial production of natural sweet wines from botrytized grapes. *American Journal of Enology and Viticulture*, 10(3): 135–141, https://doi.org/10.5344/ajev.1959.10.3.135

Pulliat, V. (1897). *Les raisins précoces pour le vinet la table*. E-book, Montpellier, France.

Rakonczás, N. (Ed.) (2014). *Viticulture*, 1st ed. University Press of Debrecen, Debrecen, Hungary.

Ross, S.M. (2010). *Introduction to probability models*. Academic Press, New York.

Seneta, E. (1966). Markov and the birth of chain dependence theory. *International Satistical Review*, 64(3): 255–263, https://doi.org/10.2307/1403785

Sonnadara, U. and Jayewardene, R. (2014). A Markov chain probability model to describe wet and dry patterns of weather at Colombo. *Theoretical and Applied Climatology*, 119(1-2): 1–16, https://doi.org/10.1007/s00704-014-1117-z

Sunarmi, N., Aisyah, W.M., Setiorini, A., Hasanah, U., Fitria, N.L., and Wati, F.K. (2022). Factor analysis on weather elements that affect marine transportation activities at Tanjung Perak Port with the principal component analysis. *Jurnal Neutrino: Jurnal Fisika dan Aplikasinya*, 15(1): 8–14, https://doi.org/10.18860/neu.v15i1.17006

Szám, D., Hetesi, Zs., Takács, A.P., Keve, G., Balling, P., and Fekete, Á. (2024). Study of drought periods in the Tokaj-Hegyalja wine region. *Progress in Agricultural Engineering Sciences*, 20(1): 113–128, https://doi.org/10.1556/446.2024.00116

Szepesi, J., Harangi, Sz., Ésik, Zs., Novák, T.J., Lukács, R., and Soós, I. (2017). Volcanic geoheritage and geotourism perspectives in Hungary: a case of an UNESCO world Heritage site, Tokaj wine region historic cultural landscape, Hungary. *Geoheritage*, 9(3): 329–349, https://doi.org/10.1007/s12371-016-0205-0

Tettey, M., Oduro, F.T., Adedida, D., and Abaye, D.A. (2017). Markov chain analysis of the rainfall patterns of five geographical locations on the south-eastern coast of Ghana. *Earth Perspectives – Transdisciplinary Enabled*, 4(6): 1–11, https://doi.org/10.1186/s40322-017-0042-6

Tosi, E., Azzolini, M., Lorenzini, M., Torriani, S., Fedrizzi, B., Finato, F., Cipriani, M., and Zapparoli, G. (2013). Induction of grape botrytization during withering affects the volatile composition of Recioto di Soave, a “passito”-style wine. *European Food Research and Technology*, 236(5): 853–862, https://doi.org/10.1007/s00217-013-1943-8

Wang, X.J., Tao, Y.S., Wu, Y., An, R.Y., and Yu, Z.Y. (2017). Aroma compounds and characteristics of noble-rot wines of Chardonnay grapes artificially botrytized in the vineyard. *Food Chemistry*, 226(1): 41–50, https://doi.org/10.1016/j.foodchem.2017.01.007

Weibull, W. (1939). The statistical theory of the strength of materials. In: *Ingeniors vetenskaps academy handlingar*. Generalstabens Litografiska Anstalts Förlag, Stockholm, Sweden, pp. 1–45.

Wilks, D.S. (1989). Rainfall intensity, the Weibull distribution, and estimation of daily surface runoff. *Journal of Applied Meteorology and Climatology*, 28(1): 52–58, https://doi.org/10.1175/1520-0450(1989)028<0052:RITWDA>2.0.CO;2

## Appendix 1. Transition probability matrices for the humidity study for the period 2002–2020 from the 10-min data series

| Season | P |
|---|---|
| 2002 | $\begin{pmatrix} 0.953 & 0.046 & 0.001 & 0.000 & 0.000 \\ 0.089 & 0.797 & 0.112 & 0.002 & 0.000 \\ 0.000 & 0.072 & 0.833 & 0.095 & 0.001 \\ 0.000 & 0.001 & 0.077 & 0.852 & 0.070 \\ 0.000 & 0.000 & 0.000 & 0.033 & 0.967 \end{pmatrix}$ |
| 2003 | $\begin{pmatrix} 0.958 & 0.041 & 0.000 & 0.000 & 0.000 \\ 0.072 & 0.858 & 0.069 & 0.001 & 0.000 \\ 0.000 & 0.067 & 0.868 & 0.065 & 0.000 \\ 0.000 & 0.000 & 0.065 & 0.901 & 0.034 \\ 0.000 & 0.000 & 0.000 & 0.042 & 0.958 \end{pmatrix}$ |
| 2004 | $\begin{pmatrix} 0.956 & 0.044 & 0.000 & 0.000 & 0.000 \\ 0.065 & 0.867 & 0.067 & 0.001 & 0.000 \\ 0.001 & 0.063 & 0.866 & 0.070 & 0.000 \\ 0.000 & 0.000 & 0.077 & 0.871 & 0.052 \\ 0.000 & 0.000 & 0.000 & 0.043 & 0.957 \end{pmatrix}$ |
| 2005 | $\begin{pmatrix} 0.946 & 0.054 & 0.001 & 0.000 & 0.000 \\ 0.059 & 0.863 & 0.077 & 0.000 & 0.000 \\ 0.000 & 0.067 & 0.873 & 0.060 & 0.000 \\ 0.000 & 0.001 & 0.063 & 0.892 & 0.044 \\ 0.000 & 0.000 & 0.000 & 0.077 & 0.923 \end{pmatrix}$ |
| 2006 | $\begin{pmatrix} 0.956 & 0.043 & 0.001 & 0.000 & 0.000 \\ 0.067 & 0.860 & 0.072 & 0.000 & 0.000 \\ 0.000 & 0.082 & 0.875 & 0.044 & 0.000 \\ 0.000 & 0.000 & 0.066 & 0.891 & 0.044 \\ 0.000 & 0.000 & 0.000 & 0.124 & 0.876 \end{pmatrix}$ |
| 2007 | $\begin{pmatrix} 0.955 & 0.044 & 0.001 & 0.000 & 0.000 \\ 0.071 & 0.838 & 0.091 & 0.001 & 0.000 \\ 0.001 & 0.079 & 0.850 & 0.071 & 0.000 \\ 0.000 & 0.002 & 0.069 & 0.908 & 0.022 \\ 0.000 & 0.000 & 0.000 & 0.064 & 0.936 \end{pmatrix}$ |
| 2008 | $\begin{pmatrix} 0.943 & 0.057 & 0.000 & 0.000 & 0.000 \\ 0.054 & 0.884 & 0.062 & 0.000 & 0.000 \\ 0.000 & 0.061 & 0.869 & 0.071 & 0.000 \\ 0.000 & 0.000 & 0.075 & 0.910 & 0.015 \\ 0.000 & 0.000 & 0.000 & 0.057 & 0.943 \end{pmatrix}$ |

*(continued)*

Continued

| Season | P |
|---|---|
| 2009 | $\begin{pmatrix} 0.972 & 0.028 & 0.000 & 0.000 & 0.000 \\ 0.059 & 0.878 & 0.063 & 0.001 & 0.000 \\ 0.001 & 0.073 & 0.851 & 0.076 & 0.000 \\ 0.000 & 0.003 & 0.063 & 0.893 & 0.041 \\ 0.000 & 0.000 & 0.000 & 0.063 & 0.937 \end{pmatrix}$ |
| 2010 | $\begin{pmatrix} 0.926 & 0.074 & 0.000 & 0.000 & 0.000 \\ 0.066 & 0.847 & 0.084 & 0.002 & 0.000 \\ 0.000 & 0.077 & 0.853 & 0.070 & 0.000 \\ 0.000 & 0.001 & 0.073 & 0.881 & 0.045 \\ 0.000 & 0.000 & 0.000 & 0.043 & 0.957 \end{pmatrix}$ |
| 2011 | $\begin{pmatrix} 0.960 & 0.040 & 0.000 & 0.000 & 0.000 \\ 0.077 & 0.844 & 0.078 & 0.001 & 0.000 \\ 0.001 & 0.086 & 0.851 & 0.062 & 0.000 \\ 0.000 & 0.001 & 0.096 & 0.874 & 0.029 \\ 0.000 & 0.000 & 0.000 & 0.081 & 0.919 \end{pmatrix}$ |
| 2012 | $\begin{pmatrix} 0.961 & 0.038 & 0.001 & 0.000 & 0.000 \\ 0.058 & 0.854 & 0.088 & 0.000 & 0.000 \\ 0.001 & 0.068 & 0.874 & 0.057 & 0.000 \\ 0.000 & 0.000 & 0.077 & 0.874 & 0.049 \\ 0.000 & 0.000 & 0.000 & 0.048 & 0.952 \end{pmatrix}$ |
| 2013 | $\begin{pmatrix} 0.958 & 0.041 & 0.001 & 0.000 & 0.000 \\ 0.066 & 0.858 & 0.076 & 0.000 & 0.000 \\ 0.001 & 0.093 & 0.848 & 0.059 & 0.000 \\ 0.000 & 0.000 & 0.071 & 0.867 & 0.062 \\ 0.000 & 0.000 & 0.000 & 0.048 & 0.952 \end{pmatrix}$ |
| 2014 | $\begin{pmatrix} 0.916 & 0.083 & 0.001 & 0.000 & 0.000 \\ 0.071 & 0.847 & 0.078 & 0.003 & 0.000 \\ 0.000 & 0.067 & 0.861 & 0.072 & 0.000 \\ 0.000 & 0.001 & 0.074 & 0.860 & 0.065 \\ 0.000 & 0.000 & 0.000 & 0.042 & 0.958 \end{pmatrix}$ |
| 2015 | $\begin{pmatrix} 0.969 & 0.031 & 0.000 & 0.000 & 0.000 \\ 0.048 & 0.894 & 0.058 & 0.000 & 0.000 \\ 0.000 & 0.051 & 0.890 & 0.059 & 0.000 \\ 0.000 & 0.001 & 0.064 & 0.898 & 0.038 \\ 0.000 & 0.000 & 0.000 & 0.031 & 0.969 \end{pmatrix}$ |
| 2016 | $\begin{pmatrix} 0.946 & 0.053 & 0.002 & 0.000 & 0.000 \\ 0.066 & 0.869 & 0.063 & 0.002 & 0.000 \\ 0.001 & 0.070 & 0.854 & 0.075 & 0.000 \\ 0.000 & 0.001 & 0.065 & 0.906 & 0.028 \\ 0.000 & 0.000 & 0.000 & 0.030 & 0.970 \end{pmatrix}$ |

*(continued)*

Continued

| Season | P |
|---|---|
| 2017 | $\begin{pmatrix} 0.945 & 0.054 & 0.001 & 0.000 & 0.000 \\ 0.066 & 0.854 & 0.079 & 0.001 & 0.000 \\ 0.001 & 0.069 & 0.857 & 0.073 & 0.001 \\ 0.000 & 0.000 & 0.072 & 0.881 & 0.047 \\ 0.000 & 0.000 & 0.000 & 0.037 & 0.962 \end{pmatrix}$ |
| 2018 | $\begin{pmatrix} 0.965 & 0.034 & 0.001 & 0.000 & 0.000 \\ 0.070 & 0.860 & 0.070 & 0.001 & 0.000 \\ 0.000 & 0.095 & 0.852 & 0.052 & 0.001 \\ 0.000 & 0.002 & 0.092 & 0.855 & 0.051 \\ 0.000 & 0.000 & 0.000 & 0.067 & 0.933 \end{pmatrix}$ |
| 2019 | $\begin{pmatrix} 0.948 & 0.051 & 0.000 & 0.000 & 0.000 \\ 0.072 & 0.850 & 0.078 & 0.000 & 0.000 \\ 0.000 & 0.092 & 0.831 & 0.076 & 0.000 \\ 0.000 & 0.002 & 0.096 & 0.848 & 0.054 \\ 0.000 & 0.000 & 0.000 & 0.061 & 0.939 \end{pmatrix}$ |
| 2020 | $\begin{pmatrix} 0.960 & 0.040 & 0.001 & 0.000 & 0.000 \\ 0.055 & 0.863 & 0.081 & 0.001 & 0.000 \\ 0.000 & 0.080 & 0.846 & 0.073 & 0.000 \\ 0.001 & 0.001 & 0.059 & 0.881 & 0.057 \\ 0.000 & 0.000 & 0.000 & 0.027 & 0.973 \end{pmatrix}$ |

Own source.

## Appendix 2. Transition probability matrices for the humidity study for the period 2002–2020 from the 60-min data series

| Season | P |
|---|---|
| 2002 | $\begin{pmatrix} 0.880 & 0.105 & 0.016 & 0.000 & 0.000 \\ 0.204 & 0.489 & 0.277 & 0.029 & 0.000 \\ 0.013 & 0.162 & 0.601 & 0.219 & 0.004 \\ 0.000 & 0.016 & 0.173 & 0.601 & 0.210 \\ 0.000 & 0.002 & 0.010 & 0.078 & 0.911 \end{pmatrix}$ |
| 2003 | $\begin{pmatrix} 0.878 & 0.110 & 0.011 & 0.000 & 0.000 \\ 0.192 & 0.612 & 0.192 & 0.004 & 0.000 \\ 0.018 & 0.175 & 0.609 & 0.186 & 0.011 \\ 0.000 & 0.007 & 0.197 & 0.677 & 0.119 \\ 0.000 & 0.000 & 0.000 & 0.158 & 0.842 \end{pmatrix}$ |
| 2004 | $\begin{pmatrix} 0.854 & 0,141 & 0.003 & 0.003 & 0.000 \\ 0.204 & 0.576 & 0.204 & 0.016 & 0.000 \\ 0.015 & 0.175 & 0.646 & 0.164 & 0.000 \\ 0.000 & 0.012 & 0.173 & 0.627 & 0.189 \\ 0.000 & 0.006 & 0.006 & 0.137 & 0.851 \end{pmatrix}$ |
| 2005 | $\begin{pmatrix} 0.852 & 0.142 & 0.006 & 0.000 & 0.000 \\ 0.158 & 0.607 & 0.208 & 0.027 & 0.000 \\ 0.003 & 0.212 & 0.615 & 0.170 & 0.000 \\ 0.000 & 0.006 & 0.191 & 0.674 & 0.129 \\ 0.000 & 0.000 & 0.000 & 0.225 & 0.775 \end{pmatrix}$ |
| 2006 | $\begin{pmatrix} 0.873 & 0.114 & 0.009 & 0.004 & 0.000 \\ 0.185 & 0.601 & 0.197 & 0.017 & 0.000 \\ 0.007 & 0.240 & 0.620 & 0.130 & 0.003 \\ 0.005 & 0.033 & 0.188 & 0.657 & 0.117 \\ 0.000 & 0.000 & 0.000 & 0.394 & 0.606 \end{pmatrix}$ |
| 2007 | $\begin{pmatrix} 0.845 & 0.142 & 0.009 & 0.002 & 0.002 \\ 0.204 & 0.576 & 0.193 & 0.026 & 0.000 \\ 0.034 & 0.151 & 0.627 & 0.188 & 0.000 \\ 0.006 & 0.009 & 0.198 & 0.719 & 0.068 \\ 0.000 & 0.000 & 0.009 & 0.202 & 0.789 \end{pmatrix}$ |
| 2008 | $\begin{pmatrix} 0.863 & 0.120 & 0.017 & 0.000 & 0.000 \\ 0.120 & 0.705 & 0.169 & 0.006 & 0.000 \\ 0.011 & 0.166 & 0.646 & 0.177 & 0.000 \\ 0.000 & 0.006 & 0.193 & 0.751 & 0.050 \\ 0.000 & 0.000 & 0.022 & 0.157 & 0.820 \end{pmatrix}$ |

*(continued)*

Continued

| Season | P |
|---|---|
| 2009 | $\begin{pmatrix} 0.903 & 0.086 & 0.009 & 0.002 & 0.000 \\ 0.201 & 0.606 & 0.166 & 0.027 & 0.000 \\ 0.009 & 0.229 & 0.601 & 0.161 & 0.000 \\ 0.000 & 0.012 & 0.160 & 0.712 & 0.115 \\ 0.000 & 0.000 & 0.012 & 0.152 & 0.836 \end{pmatrix}$ |
| 2010 | $\begin{pmatrix} 0.811 & 0.185 & 0.004 & 0.000 & 0.000 \\ 0.152 & 0.625 & 0.202 & 0.022 & 0.000 \\ 0.013 & 0.182 & 0.607 & 0.195 & 0.003 \\ 0.000 & 0.013 & 0.185 & 0.662 & 0.140 \\ 0.000 & 0.000 & 0.021 & 0.116 & 0.862 \end{pmatrix}$ |
| 2011 | $\begin{pmatrix} 0.886 & 0.101 & 0.013 & 0.000 & 0.000 \\ 0.201 & 0.594 & 0.179 & 0.025 & 0.000 \\ 0.014 & 0.205 & 0.627 & 0.144 & 0.010 \\ 0.005 & 0.038 & 0.240 & 0.623 & 0.093 \\ 0.000 & 0.000 & 0.015 & 0.292 & 0.692 \end{pmatrix}$ |
| 2012 | $\begin{pmatrix} 0.880 & 0.105 & 0.013 & 0.003 & 0.000 \\ 0.158 & 0.619 & 0.211 & 0.012 & 0.000 \\ 0.021 & 0.150 & 0.665 & 0.147 & 0.018 \\ 0.000 & 0.012 & 0.215 & 0.622 & 0.150 \\ 0.000 & 0.000 & 0.008 & 0.167 & 0.824 \end{pmatrix}$ |
| 2013 | $\begin{pmatrix} 0.877 & 0.112 & 0.011 & 0.000 & 0.000 \\ 0.190 & 0.634 & 0.166 & 0.003 & 0.007 \\ 0.008 & 0.223 & 0.618 & 0.147 & 0.004 \\ 0.000 & 0.000 & 0.187 & 0.622 & 0.192 \\ 0.000 & 0.000 & 0.019 & 0.134 & 0.847 \end{pmatrix}$ |
| 2014 | $\begin{pmatrix} 0.785 & 0.190 & 0.020 & 0.005 & 0.000 \\ 0.171 & 0.583 & 0.217 & 0.029 & 0.000 \\ 0.010 & 0.190 & 0.588 & 0.190 & 0.021 \\ 0.000 & 0.017 & 0.203 & 0.624 & 0.155 \\ 0.000 & 0.002 & 0.007 & 0.107 & 0.884 \end{pmatrix}$ |
| 2015 | $\begin{pmatrix} 0.880 & 0.112 & 0.008 & 0.000 & 0.000 \\ 0.175 & 0.654 & 0.167 & 0.004 & 0.000 \\ 0.011 & 0.137 & 0.690 & 0.162 & 0.000 \\ 0.000 & 0.008 & 0.169 & 0.679 & 0.144 \\ 0.000 & 0.003 & 0.003 & 0.108 & 0.886 \end{pmatrix}$ |
| 2016 | $\begin{pmatrix} 0.850 & 0.144 & 0.006 & 0.000 & 0.000 \\ 0.162 & 0.632 & 0.173 & 0.029 & 0.004 \\ 0.019 & 0.189 & 0.598 & 0.193 & 0.000 \\ 0.003 & 0.007 & 0.185 & 0.708 & 0.097 \\ 0.000 & 0.000 & 0.004 & 0.102 & 0.895 \end{pmatrix}$ |

*(continued)*

Continued

| Season | P |
| --- | --- |
| 2017 | $\begin{pmatrix} 0.824 & 0.163 & 0.013 & 0.000 & 0.000 \\ 0.197 & 0.531 & 0.238 & 0.029 & 0.004 \\ 0.018 & 0.213 & 0,557 & 0.202 & 0.011 \\ 0.000 & 0.011 & 0.208 & 0.647 & 0.134 \\ 0.000 & 0.000 & 0.017 & 0.100 & 0.883 \end{pmatrix}$ |
| 2018 | $\begin{pmatrix} 0.883 & 0.101 & 0.011 & 0.005 & 0.000 \\ 0.219 & 0.607 & 0.165 & 0.009 & 0.000 \\ 0.013 & 0.260 & 0.591 & 0.119 & 0.017 \\ 0.000 & 0.029 & 0.235 & 0.574 & 0.162 \\ 0.000 & 0.000 & 0.018 & 0.220 & 0.761 \end{pmatrix}$ |
| 2019 | $\begin{pmatrix} 0.846 & 0.143 & 0.009 & 0.002 & 0.000 \\ 0.184 & 0.598 & 0.196 & 0.018 & 0.003 \\ 0.032 & 0.218 & 0.554 & 0.182 & 0.014 \\ 0.005 & 0.020 & 0.283 & 0.546 & 0.146 \\ 0.000 & 0.000 & 0.000 & 0.177 & 0.823 \end{pmatrix}$ |
| 2020 | $\begin{pmatrix} 0.858 & 0.138 & 0.004 & 0.000 & 0.000 \\ 0.185 & 0.555 & 0.237 & 0.024 & 0.000 \\ 0.005 & 0.251 & 0.543 & 0.191 & 0.010 \\ 0.000 & 0.016 & 0.152 & 0.658 & 0.175 \\ 0.000 & 0.000 & 0.004 & 0.087 & 0.909 \end{pmatrix}$ |

Own source.